Journal of Digital Imaging

One Year's Results from a Server-Based System for Performing Reject Analysis and Exposure Analysis in Computed Radiography

A. Kyle Jones,[1] Raimund Polman,[1] Charles E. Willis,[1] and S. Jeff Shepard[1]

Rejected images represent both unnecessary radiation exposure to patients and inefficiency in the imaging operation. Rejected images are inherent to projection radiography, where patient positioning and alignment are integral components of image quality. Patient motion and artifacts unique to digital image receptor technology can result in rejected images also. We present a centralized, server-based solution for the collection, archival, and distribution of rejected image and exposure indicator data that automates the data collection process. Reject analysis program (RAP) and exposure indicator data were collected and analyzed during a 1-year period. RAP data were sorted both by reason for repetition and body part examined. Data were also stratified by clinical area for further investigation. The monthly composite reject rate for our institution fluctuated between 8% and 10%. Positioning errors were the main cause of repeated images (77.3%). Stratification of data by clinical area revealed that areas where computed radiography (CR) is seldom used suffer from higher reject rates than areas where it is used frequently. *S* values were log-normally distributed for examinations performed under either manual or automatic exposure control. The distributions were positively skewed and leptokurtic. *S* value decreases due to radiologic technology student rotations, and CR plate reader calibrations were observed. Our data demonstrate that reject analysis is still necessary and useful in the era of digital imaging. It is vital though that analysis be combined with exposure indicator analysis, as digital radiography is not self-policing in terms of exposure. When combined, the two programs are a powerful tool for quality assurance.

KEY WORDS: Computed radiography, data collection, data mining, quality assurance, quality control, radiography, statistic analysis, radiation dose, reject analysis, repeat analysis, exposure analysis

INTRODUCTION

Repeated and rejected images represent both unnecessary radiation exposure to patients and inefficiency in the imaging operation owing to wasted time and resources. Repeated images are inherent to projection radiography, where patient positioning and alignment are integral components of image quality. With screen–film imaging systems, the relatively narrow exposure latitude available for creating a clinically useful image sometimes necessitates repeated images owing to under- or overexposure of the film. Patient motion and artifacts unique to the image receptor technology can result in repeated images as well. Therefore, repeat/reject analysis is an integral part of a quality assurance (QA) program for radiography. Repeat/reject analysis is mandated by the US government for mammography[1] and is recommended for projection radiography by multiple organizations and accrediting bodies.[2–4]

In screen–film imaging departments, reject analysis programs (RAP) rely on the physical collection of rejected images in containers, the contents of which are periodically sorted by reason for rejection and normalized by the total number of films consumed during the period to determine reject rates.[5] This system is often complicated by the time-consuming task of determining reasons for rejection "after the fact" and determining the total number of films consumed.[6]

[1]From the Department of Imaging Physics, The University of Texas M. D. Anderson Cancer Center, 1515 Holcombe Blvd., Unit 1352, Houston, TX, 77030, USA.

Correspondence to: A. Kyle Jones, Department of Imaging Physics, The University of Texas M. D. Anderson Cancer Center, 1515 Holcombe Blvd., Unit 1352, Houston, TX, 77030, USA; tel: +1-713-5630552; fax: +1-713-5638842; e-mail: kyle.jones@mdanderson.org

Online publication 3 November 2009
doi: 10.1007/s10278-009-9236-2

During early clinical experience with digital radiography, it was proposed that this new technology might eliminate repeated images and render any RAP obsolete.[7] However, imaging departments quickly realized that this was not the case[8] and that a RAP was still a vital part of a QA program. In fact, digital radiography has made reject analysis more complicated and, ironically, may facilitate the repetition of images owing to the ease of acquisition, especially with cassette-less systems where no manual intervention occurs between receptor exposure and image readout. Physical evidence of rejected images no longer exists for tallying, and on many early digital imaging systems, radiographers can simply delete unwanted images, which are ultimately never accounted for.[8,9] This is still a problem today, and one manufacturer of indirect digital radiography (iDR) equipment whose equipment is installed at our institution allows the user to select "Delete" from a right-click pop-up menu during an active examination unless the function is locked by the administrator. Even if deletion is not an option, rejected images often simply reside in the system until they are deleted to make room for more images.

Thus, the adoption of digital imaging and specifically soft-copy interpretation forced radiology departments to develop innovative RAP. Early methods used for RAP included manual collection of data from acquisition stations,[10,11] manual tagging of rejected images by a QA radiologic technologist (RT),[9] manipulation of examination and demographic information in rejected images along with the use of routing tables to segregate rejected images,[8] and extraction of information from the Digital Imaging and Communications in Medicine (DICOM) header.[12] Most of these methods involved manual collection of data and were subject to similar problems, including lack of RT compliance,[8–10] intentional circumvention of the program by RTs,[9] accidental deletion of data,[11] and false-negative or false-positive results.[12] Recently, two studies have described sophisticated server-based RAPs that automatically collect, parse, and analyze data from many different acquisition systems spread throughout an institution.[13,14] These types of RAPs avoid many of the difficulties associated with manual data collection and analysis.

Perhaps as important as the RAP is a program to track exposures in digital imaging departments. Burkhart proposed that ongoing study of the retake rate and its causes is the most useful means of evaluating the effectiveness of a quality assurance program.[15] Others have argued that monitoring image quality and patient exposures are all that is necessary in a quality assurance program, and in the era of digital imaging, deeper investigation of equipment operating parameters should be performed only when either is out of tolerance (Gray 2008, personal communication). Exposures in screen–film departments were indirectly monitored via the optical density of resultant films: Underexposed films were light and overexposed films were dark. These films were then sent to the reject bin, where they were counted as part of the RAP. Digital imaging has resulted in the decoupling of receptor exposure and the related quantity of patient exposure from the grayscale appearance of the electronic image. While this has resulted in fewer repeats due to overexposed images,[9–11,16] it has also resulted in a phenomenon known as dose creep.[17,18] Because of the automatic adjustment of grayscale in digital imaging, until the limit of adjustment is reached, overexposed images have a more pleasing appearance than underexposed images. Technologists respond to feedback from radiologists who naturally prefer less noisy images. Thus, receptor exposures tend to increase over time, and consequently, patient exposures also increase. Therefore, it is important to monitor exposures to maintain a level that provides adequate image quality at a radiation exposure that is as low as reasonably achievable. Previous reports demonstrated the ability to tighten exposure ranges and reduce the number and frequency of overexposures.[19,20]

Our institution has a large installed base of FujiFilm (FujiFilm Medical Systems, Stamford, CT, USA) computed radiography (CR) equipment. FujiFilm provides several utilities in the form of graphical user interfaces on their Intelligent Image Processing (IIP) workstations that enable an authorized user to download rejected image data and exposure indicator data. The results can be downloaded in comma-separated values (CSV) format to a 3.5-in. floppy disk or Universal Serial Bus portable media for further analysis. However, several problems exist with this method of data collection. First, as mentioned earlier, the data must be retrieved manually. This task can be quite burdensome, particularly if an institution is dispersed among multiple buildings that are geographically separated. For example, our institution has 27 IIP stations distributed across several buildings, separated by as much as 1/2 mile. Second, accidental or intentional deletion of data can occur, frequently by unwitting service engineers, resulting in data collection gaps. Finally, cobbling the data from multiple systems into one usable format can be challenging.

We believed that we could implement a combined RAP and EAP while addressing long-standing problems with rejected image analysis using readily available resources and tools. To this end, we developed a centralized, server-based solution for the collection, archival, and distribution of RAP and exposure indicator data that automate the data collection process. Our process does require some human intervention: initially to configure acquisition stations to download data and ongoing selection of reasons for rejection of an image. In its current state, our system still relies upon humans to analyze the data, which is a limitation. However, future versions will incorporate automated analysis into the process.

MATERIALS AND METHODS

This report is based solely on our experience with FujiFilm equipment. In our clinical setting, most projection radiography is accomplished by iDR, and cassette-based CR is used primarily for bedside examinations and those views that are inconvenient for our iDR systems. However, our methods and techniques should translate easily to other systems. Our radiologic technologists were aware that rejected image analysis and exposure analysis were being performed during the course of this study.

We used an existing server running SUSE Linux 10.0 (Novell, Waltham, MA, USA). An MS-DOS batch file that executes the necessary commands to download RAP and exposure indicator data was installed on each IIP at our institution, and the downloaded data were transferred via FTP to our central server. This process was executed each day at midnight using a scheduled task in the Windows operating system on the IIP and crontab, a job scheduler in Unix and Linux operating systems, on the server side. Administrators were automatically notified via email of any errors encountered during the process to ensure contiguous collection of data. Additional data, including technologist identification number and name, were then collected from the Radiology Information System (RIS) to complete the assembly of our data set (Table 1). Technologists were linked to rejected images by the accession number of the examination. All data were parsed into a MySQL (MySQL AB, Uppsala, Sweden) database after collection. Server-side programming was implemented in Practical Extraction and Report Language.[21]

Exposure indicator data for each view were collected in a similar fashion. The exposure indicator reported by FujiFilm CR systems is the S value. The S value is related to the exposure incident on an imaging plate as

$$S \approx \frac{200}{X}, \qquad (1)$$

where X is the exposure (mR) incident on the imaging plate. The L value, which corresponds to the number of decades of exposure digitized in the final image, is also included in the collected exposure analysis data. The accuracy of the S value and its relationship to patient exposure is dependent upon many factors, including exposure conditions, patient positioning, algorithm selection, and patient body habitus.

S value data were analyzed and results presented using descriptive statistics. It is worthwhile to discuss the statistical analysis of S value data. It has been shown previously that S value data for examinations performed under manual exposure control are not normally distributed but instead are log-normally distributed, as illustrated in Figure 1.[22] This distribution arises because the X-ray beam incident on the CR plate has been exponentially attenuated while passing through the patient, and patient thickness is normally distributed. Therefore, we performed a log transform on S value data prior to analysis, then an antilog transform to prepare the data for presentation. Statistical descriptors were calculated appropriately given the log-normal distribution[23]:

$$\mu_{S\#} = \exp\left(\mu_{\log(S\#)} + \frac{\sigma^2_{\log(S\#)}}{2}\right), \qquad (2)$$

$$\mathrm{median}_{S\#} = \exp\left(\mu_{\log(S\#)}\right), \qquad (3)$$

$$\mathrm{mode}_{S\#} = \exp\left(\mu_{\log(S\#)} - \sigma^2_{\log(S\#)}\right), \qquad (4)$$

Table 1. Data Stored in mySQL Database for Rejected Image Analysis and Exposure Analysis

Field	Function	Necessary data?
Acquisition station	Can identify specific stations with problems	–[a]
Accession number	Links study to technologist through RIS	–[a]
Exam date	Allows sorting of data by month	–[a]
Body part	Allows sorting of data by body part	–[a]
View	Allows sorting of data by view	–[a]
Exposure indicator	Allows exposure analysis	–[a]
Reject category	Allows reject analysis	–[a]
Reject comments	Further clarifies reason for rejection-free field	
Technologist ID	Alternative method of linking technologist and study	
Technologist name	Allows sorting of data by technologist name	
Thumbnail image	Verification of reason for rejection	

[a]Denotes what we consider to be minimum necessary data for RAP and EAP

$$\text{skewness}_{S\#} = \left[\exp\left(\sigma^2 + 2\right) \times \sqrt{\exp\left(\sigma^2\right) - 1}\right], \text{ and} \quad (5)$$

$$\text{kurtosis}_{S\#} = \exp\left(4\sigma^2\right) + 2\exp\left(3\sigma^2\right) + 3\exp\left(2\sigma^2\right) - 6. \quad (6)$$

Outliers in the transformed S value data were eliminated according to Chauvenet's criterion.[24]

Currently, authorized users can access RAP and exposure indicator data hosted on an Apache web server (The Apache Software Foundation, Forest Hill, MD, USA) via an HTTP web interface (Fig. 2) from any computer within the Division of Diagnostic Imaging intranet. Access is password protected on two levels, one via departmental intranet authentication and the second via a user account on the Apache server. From this interface, the user can filter data by month, year, and clinical location within Diagnostic Imaging. Pages are dynamically generated using Common Gateway Interface. In addition, a feature allows the inclusion or exclusion of student data. From this interface, the user can peruse the data, view rejected images in JPEG format, or download data in CSV format for further analysis.

An exposure indicator log is also accessible via a similar HTTP interface (Fig. 3). This HTTP interface also affords access to other information, including L value and plate ID, from every image that has been acquired. While this feature is less useful for visual analysis, it is very powerful for downloading large amounts of exposure data in CSV format for analysis of exposure trends.

RAP and exposure indicator data were collected for 12 months, from April 2007 to March 2008. RAP data were sorted both by reason for rejection and body part examined, as previously recommended.[25] Data were also stratified by clinical location for further investigation. In addition, data from our exposure analysis program (EAP) were analyzed

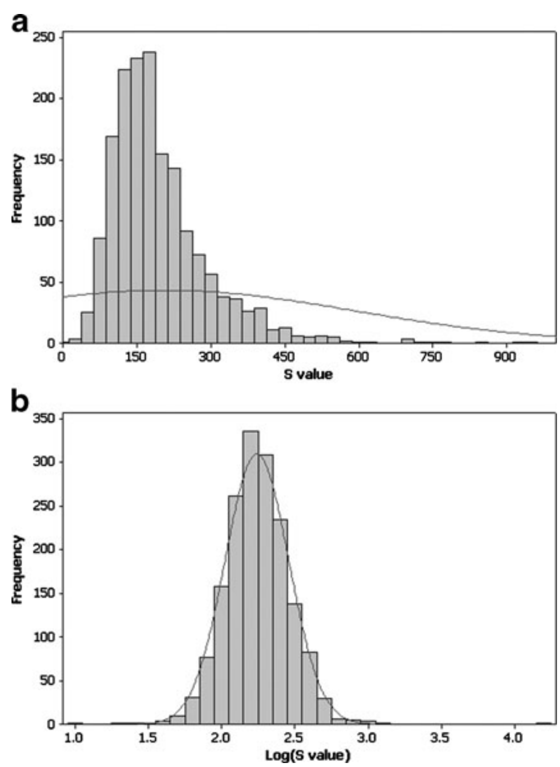

Fig 1. a S values are poorly characterized by the normal distribution, while b log(S value) is well-fit by the normal distribution.

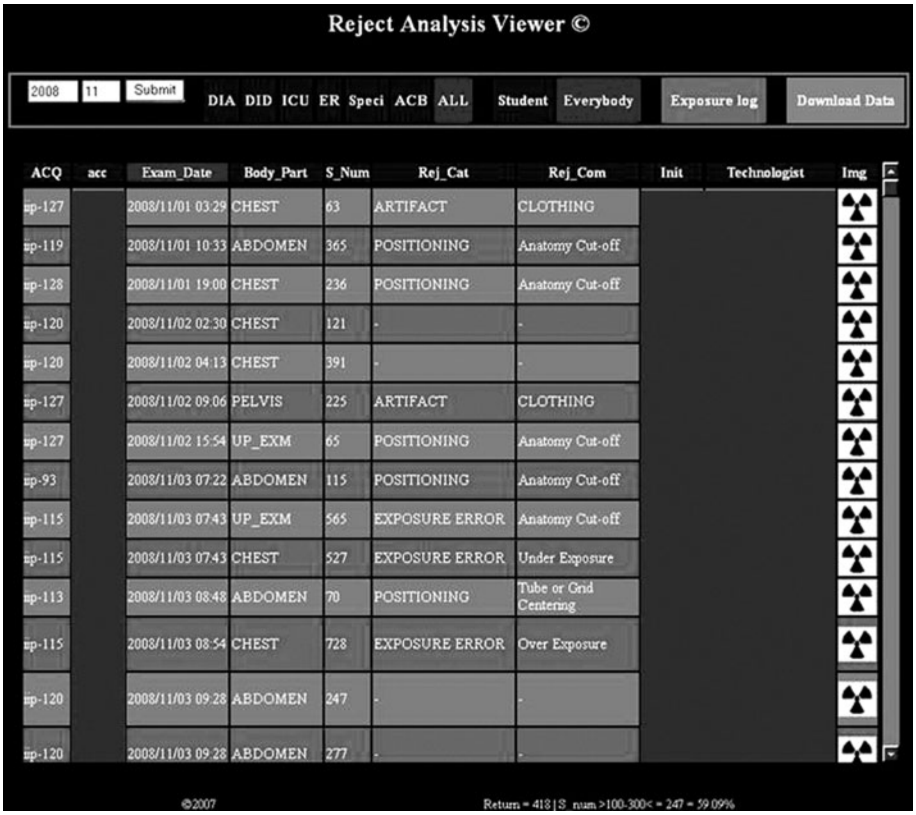

ACQ	acc	Exam_Date	Body_Part	S_Num	Rej_Cat	Rej_Com	Init	Technologist	Img
ip-127	[redacted]	2008/11/01 03:29	CHEST	63	ARTIFACT	CLOTHING	[redacted]	[redacted]	
ip-119	[redacted]	2008/11/01 10:33	ABDOMEN	365	POSITIONING	Anatomy Cut-off	[redacted]	[redacted]	
ip-128	[redacted]	2008/11/01 19:00	CHEST	236	POSITIONING	Anatomy Cut-off	[redacted]	[redacted]	
ip-120	[redacted]	2008/11/02 02:30	CHEST	121	-	-	[redacted]	[redacted]	
ip-120	[redacted]	2008/11/02 04:13	CHEST	391	-	-	[redacted]	[redacted]	
ip-127	[redacted]	2008/11/02 09:06	PELVIS	225	ARTIFACT	CLOTHING	[redacted]	[redacted]	
ip-127	[redacted]	2008/11/02 15:54	UP_EXM	65	POSITIONING	Anatomy Cut-off	[redacted]	[redacted]	
ip-93	[redacted]	2008/11/03 07:22	ABDOMEN	115	POSITIONING	Anatomy Cut-off	[redacted]	[redacted]	
ip-115	[redacted]	2008/11/03 07:43	UP_EXM	565	EXPOSURE ERROR	Anatomy Cut-off	[redacted]	[redacted]	
ip-115	[redacted]	2008/11/03 07:43	CHEST	527	EXPOSURE ERROR	Under Exposure	[redacted]	[redacted]	
ip-113	[redacted]	2008/11/03 08:48	ABDOMEN	70	POSITIONING	Tube or Grid Centering	[redacted]	[redacted]	
ip-115	[redacted]	2008/11/03 08:54	CHEST	728	EXPOSURE ERROR	Over Exposure	[redacted]	[redacted]	
ip-120	[redacted]	2008/11/03 09:28	ABDOMEN	247	-	-	[redacted]	[redacted]	
ip-120	[redacted]	2008/11/03 09:28	ABDOMEN	277	-	-	[redacted]	[redacted]	

Fig 2. Screen capture from HTTP interface to RAP database. Sensitive information has been blocked out. Symbols in right-most column normally appear as JPEG thumbnails of rejected images.

for the same time period using descriptive statistics and single-tailed, two-sample *t* tests.

RESULTS AND DISCUSSION

RAP Data

Overall, 6,002 images were rejected out of a total of 66,063. Figure 4 presents the monthly composite reject rate, defined as the ratio of the number of rejected images to the total number of images acquired, institution-wide. The reject rate at our institution generally fluctuated between 8% and 10% and dipped slightly below 8% during December 2007 and February 2008. The mean rate was 8.7%, and all monthly rates fell within 2 standard deviations of the mean (7.2%<×<10.3%). When the reject rate was stratified by clinical area, more variation was seen (Fig. 5a). This variation is depicted in Figure 5b, which plots the number of CR exposures performed in each clinical area per month. The total number of exposures was derived from exposure indicator logs, which recorded an *S* value for each image acquired, whether accepted or rejected. Taken as a whole, Figure 5 demonstrates that clinical areas where few cassette-based examinations were performed suffered from the highest reject rates, whereas areas that frequently used cassette-based CR were characterized by lower reject rates. For example, area 1 is predominantly an outpatient imaging area, using five iDR systems and one radiographic/fluoroscopic system. Cassette-based CR is used only for scout films during cystogram studies and for decubitus images on the iDR systems. Area 1 had the highest reject rate of any clinical area. Conversely, area 5 is the intensive care unit, where many bedside radiographic examinations are performed each day, and it had the lowest reject rate of any clinical area.

The reasons for rejection available for technologist selection were the default reasons installed on our IIPs: POSITIONING, PATIENT ID,

Fig 3. Screen capture of EAP interface. Sensitive information has been blocked out.

EXPOSURE ERROR, TEST IMAGES, and ARTIFACT. A blank field was also provided, and we have classified this selection as NONE. Technologists did have the option of selecting a secondary reason or adding comments in a free text field to further refine the cause; however, these responses were not included in this study. Table 2 stratifies rejected images by reason for rejection. As reported by previous studies,[8–13,16] the majority of rejected images were due to positioning errors (4,639 images, 77.3%), and only 9.8% (588) were rejected owing to exposure errors. Of the 588 rejects classified as EXPOSURE ERROR, 31.8% (187) were actually within our institution's acceptable range of S=50 to S=500. Furthermore, 13.6% (80) of the EXPOSURE ERROR rejects were characterized by S=200 and L=4.0, which resulted when the CR system detected insufficient light output during the scanning process. This can result from a gross underexposure of a clinical image, the reading of an unexposed cassette, or exposure of the patient without the cassette in the X-ray field. Therefore, these rejects were classified as underexposures. The 68.2% of rejects (401) marked correctly as EXPOSURE ERROR, along with those characterized by S=200 and L=4.0, were classified as underexposures (329 images, 82.0%) and overexposures (72 images, 18.0%). Fifty images

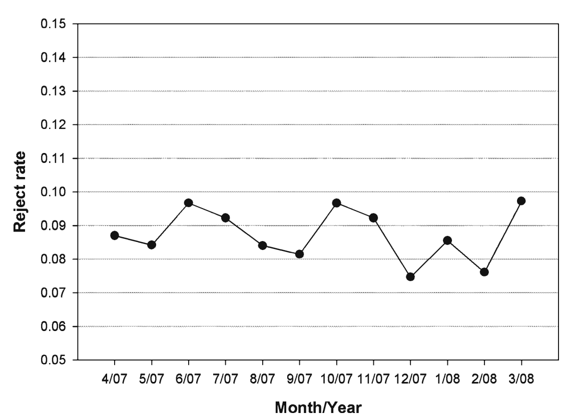

Fig 4. Composite, institution-wide reject rate for CR imaging over 1 year.

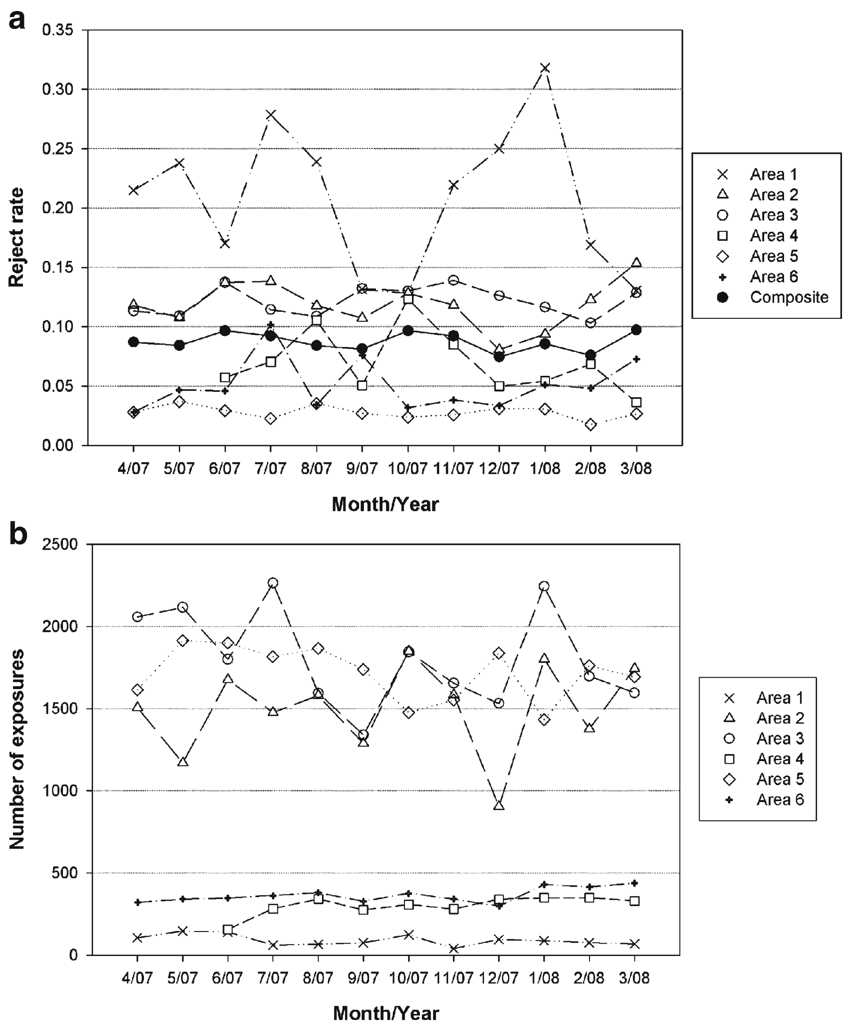

Fig 5. a Monthly reject rate stratified by clinical area. b Number of exposures per month stratified by clinical area. Note that the area that performs the fewest CR exposures (area 1) has the highest reject rate.

(0.8%) were rejected owing to "Patient ID". This was surprising considering that our institution uses DICOM Modality Worklist (MWL) for automated association of demographic information with images; however, errors unique to DICOM MWL can still occur, such as incorrect patient selection from the worklist.[26] Demographic information errors in digital imaging can and should be corrected electronically during or after the procedure, resulting in the elimination of these types of errors. It is possible that images marked incorrectly with lead markers could have been mistakenly placed in this category instead of the "Positioning" category.

Table 3 stratifies rejected image data by view. The view was derived from the menu code field stored by the IIP reject analysis interface. This breakdown is more useful than a breakdown by body part examined, as many views can be included for one body part. For example, on the FujiFilm CR system, the body part denoted as CHEST contains not only chest images but also

Table 2. Number of Rejected Images According to Reason for Rejection

Reason for rejection	Number of rejects	Percentage of rejects
Positioning	4,639	77.3
Exposure Error	588	9.8
None	571	9.5
Artifact	100	1.7
Test Images	54	0.9
Patient ID	50	0.8
Totals	6,002	100

Table 3. Rejected Images According to Intelligent Imaging Processing Menu Code

Menu code	Total images	Percentage of images	Total rejects	Percentage rejected	Percentage of total rejects
ABDOMEN, LT. DECUB	5,769	8.7	821	14.2	13.7
CHEST PORTABLE	26,400	40.0	799	3.0	13.3
ABDOMEN, GENERAL	6,177	9.4	617	10.0	10.3
ABDOMEN, RT. DECUB	3,024	4.6	470	15.5	7.8
PELVIS, GENERAL	1,650	2.5	311	18.8	5.2
CHEST, DECUBITUS	968	1.5	293	30.3	4.9
HUMERUS	1,532	2.3	191	12.5	3.2
THORACIC SPINE, LATERAL	691	1.0	184	26.6	3.1
FEMUR, PROXIMAL	1,687	2.6	157	9.3	2.6
RIBS, UPPER OBLIQUE	841	1.3	156	18.5	2.6
TIBIA/FIBULA	1,948	2.9	145	7.4	2.4
SCAPULA, "Y" VIEW	377	0.6	139	36.9	2.3
FEMUR, DISTAL	1,903	2.9	136	7.1	2.3
LUMBAR SPINE, LATERAL	751	1.1	117	15.6	1.9
SHOULDER	613	0.9	84	13.7	1.4
ABDOMEN, HIGH/LOW	513	0.8	79	15.4	1.3
ANKLE	782	1.2	71	9.1	1.2
RIBS, LOWER	498	0.8	69	13.9	1.1
KNEE, AP/OBLIQUE	553	0.8	68	12.3	1.1
KNEE, LATERAL	487	0.7	64	13.1	1.1
LUMBAR SPINE, AP/OBLIQUE	614	0.9	63	10.3	1.0
CERVICAL, LATERAL	524	0.8	61	11.6	1.0
HIP, FROG-LEG	596	0.9	59	9.9	1.0
RIBS, UPPER	432	0.7	58	13.4	1.0
THORACIC SPINE, AP	535	0.8	58	10.8	1.0
CERVICAL SPINE	216	0.3	53	24.5	0.9
FOOT	609	0.9	51	8.4	0.8
HAND	501	0.8	50	10.0	0.8
WRIST	511	0.8	47	9.2	0.8
SKULL, LATERAL	378	0.6	46	12.2	0.8
TO Lateral Pelvis[a]	131	0.2	46	35.1	0.8
FOREARM	990	1.5	44	4.4	0.7
ABDOMEN, S.B.F.T.	598	0.9	37	6.2	0.6
HIP	480	0.7	37	7.7	0.6
RECTUM, PA	330	0.5	30	9.1	0.5
HAND, LATERAL	181	0.3	28	15.5	0.5
ELBOW	269	0.4	25	9.3	0.4
FOOT, LATERAL	249	0.4	24	9.6	0.4
CLAVICLE/AC JOINTS	86	0.1	22	25.6	0.4
HAND, FINGERS	103	0.2	15	14.6	0.2
MANDIBLE, OBLIQUE	22	0.0	11	50.0	0.2
SKULL, AP/PA	61	0.1	10	16.4	0.2
CERVICAL, C7-T1 SWIMMERS	56	0.1	9	16.1	0.1
SACRUM/COCCYX, SI JOINTS	29	0.0	9	31.0	0.1
ABD. B.E. AIR CONTRAST	92	0.1	8	8.7	0.1
SCAPULA, AP	41	0.1	8	19.5	0.1
CHEST, PA	41	0.1	3	7.3	0.0

Note: Any menu code with fewer than 34 examinations is not included. When rounded, these comprise 0.0% of the total number of images acquired

[a]Cross-table pelvis image to assess position of tandem and ovoid applicators placed in operating room

views of the ribs, clavicle, sternum, etc. Table 4 shows both the percentage that each view comprised of the total number of rejected images and the percentage that each view was rejected relative to the total number of times that specific view was acquired. These data tend to parallel the clinical area data seen in Figure 5, but in this case demonstrate that a specific view that is rarely performed is frequently rejected, likely owing to lack of experience on the part of the technologists.

Table 4. Fuji *S* Value Statistics by Type of Examination—More Than 1,000 Examinations Each Performed

Examination	*S* value target	Mean (1 SD)	COV	Median	Mode
CHEST, PORTABLE	200	188.5 (77.5)	0.41	174	149
ABDOMEN, GENERAL	200	156.2 (87.1)	0.56	136	104
ABDOMEN, LEFT DECUB	200	200.8 (102.5)	0.51	179	142
ABDOMEN, RIGHT DECUB	200	219.3 (100.0)	0.46	200	165
TIB/FIB	100	191.1 (103.6)	0.54	168	130
FEMUR, DISTAL	100	152.2 (48.7)	0.32	145	131
FEMUR, PROXIMAL	200	188.5 (71.0)	0.38	176	155
HUMERUS	100	186.3 (100.9)	0.48	164	127
PELVIS, GENERAL	200	163.1 (77.9)	0.54	147	120

EAP Data

Figure 6 presents monthly exposure indicator data for body part examined ABDOMEN. Although ABDOMEN includes several views (GENERAL, LT DECUB, RT DECUB), these examinations are all very closely related, utilize similar radiographic techniques, and have the same target *S* value at our institution (*S*=200), therefore analyzing these composite data is still potentially useful. Figure 6a plots three statistical descriptors—mean, median, and mode, and Figure 6b plots the mean ±1 standard deviation. The data exhibit characteristics of the log-normal distribution: Their distribution is positively skewed, and their mean is greater than the median, which is in turn greater than the mode. The average skewness of the distribution is 1.78 and the distribution is highly

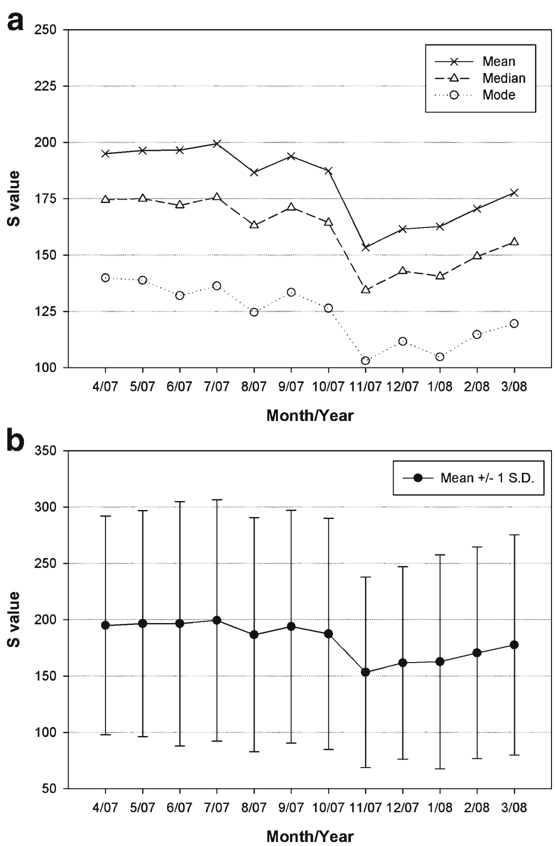

Fig 6. Statistical analysis of *S* values over a year period for body part examined ABDOMEN: a mean, median, and mode; b mean±1 standard deviation.

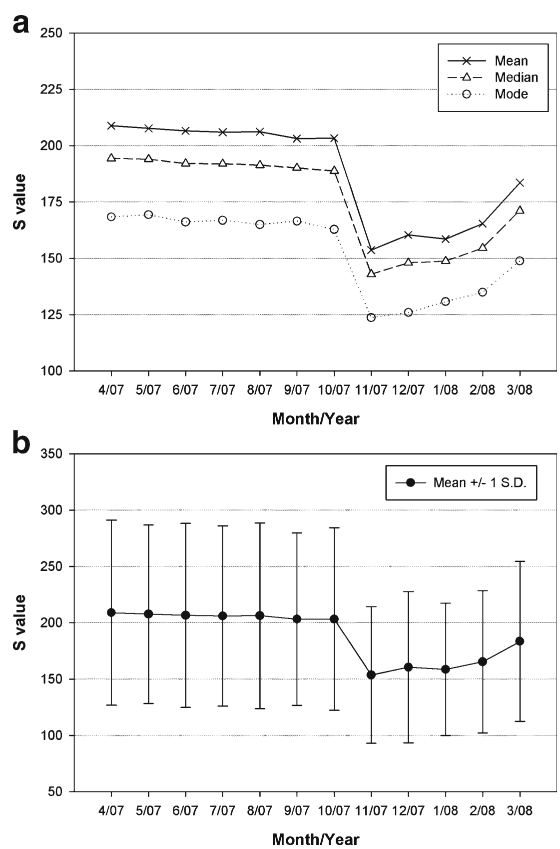

Fig 7. Statistical analysis of *S* values over a year period for view PORTABLE CHEST: a mean, median, and mode; b mean±1 standard deviation.

leptokurtic (kurtosis=6.16). When the data are viewed longitudinally, it is interesting to note that a highly significant ($p<0.001$) 15–20% decrease in *S* value occurred from October 2007 to November 2007. We attributed this decrease solely to the introduction of new radiologic technologist students into the clinic, as the *S* values for examinations included in the body part examined ABDOMEN performed by students were significantly less than those performed by employees ($p<0.01$).

Similar data for the view PORTABLE CHEST, a single view using only manual exposure control, are shown in Figure 7. The *S* value distribution is log-normal, positively skewed (1.23), and leptokurtic (2.82). Again, a highly significant ($p<0.001$) 15–20% decrease in *S* value, corresponding to higher exposures, was seen from October 2007 to November 2007. However, in this case, *S* values for PORTABLE CHEST examinations performed by students were not significantly less than those performed by employees ($p=0.84$). Therefore, the decrease in *S* values from October 2007 to November 2007 must have been influenced by other factors than just the introduction of new students into the clinic. A review of quality control records revealed that *S* value calibrations were performed on several CR plate reader units that were heavily used for reading bedside examinations, including the view PORTABLE CHEST. These calibrations resulted in an average *S* value decrease of 60 for an exposure of 1 mR to the imaging plate. Therefore, the use of similar manual exposure techniques after the calibration would have resulted in decreased S values. It can be seen that the impact of reader calibrations on exposures can be long-lasting, as the mean and median *S* values had not returned to baseline after 5 months (Fig. 7b).

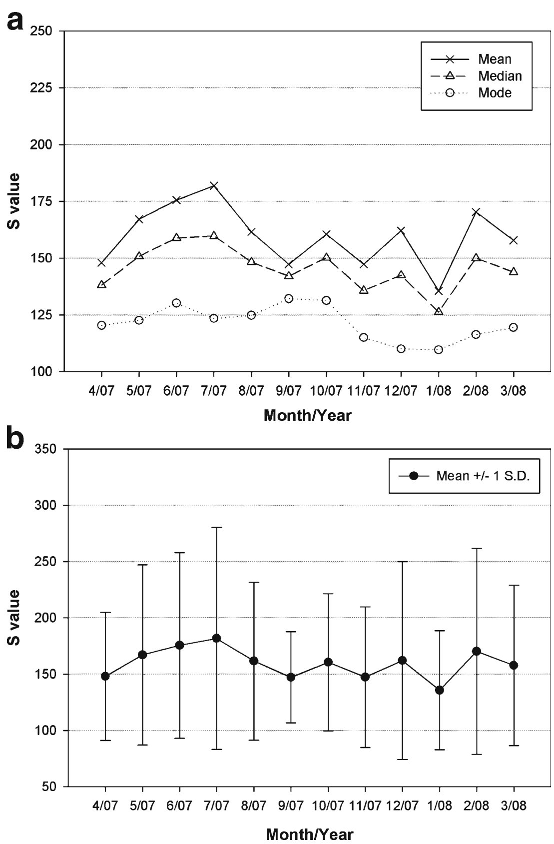

Fig 8. Statistical analysis of *S* values over a year period for view PELVIS, GENERAL: a mean, median, and mode; b mean±1 standard deviation.

Monthly exposure data for the view PELVIS, GENERAL are presented in Figure 8. This view is comprised almost exclusively of images acquired under automatic exposure control (AEC). It is important to note that the data appear to be described well by the log-normal distribution, evidenced by the hierarchy of mean, median, and mode and a positively skewed (1.42) and leptokurtic (3.96) distribution. More month-to-month variation was seen in these data (Fig. 8a), including a decrease in *S* value from October 2007 to November 2007. The observed decrease was not as drastic as seen for other views, but was significant ($p<0.05$). However, other significant fluctuations occurred during the year: A significant decrease in mean *S* value occurred from December 2007 to January 2008 ($p<0.05$) and a highly significant increase in mean *S* value occurred from January 2008 to February 2008 ($p<0.01$). Much of this variation may relate to the dependence of *S* values of images acquired under AEC on two separate pieces of equipment—the CR plate reader and the radiographic system, especially the AEC system. We did not perform sensitivity calibrations on our AEC systems during the time of this study; however, we did adjust the balance of the AEC system when found to be out of tolerance during the course of annual quality control testing. Pelvis images at our institution are acquired under AEC using the left and right AEC cells, and therefore, a rebalancing of the cells, which is usually referenced to the center cell, would change the exposures delivered to CR plates. This is difficult to confirm due to lag time between quality control

Table 5. Fuji *S* Value Statistics for Abdomen, General, Stratified by Clinical Area

Area	Exposure control	Number performed	Mean (1 S.D.)	COV	Median	Mode
1	Automatic	434	144.5 (36.2)	0.25	140	132
2	Automatic	1,717	135.3 (67.3)	0.50	121	97
3	Automatic	1,149	121.6 (61.6)	0.51	109	86
5	Manual	1,713	191.5 (105.3)	0.55	168	129

testing and corrective action and because our CR systems are not integrated, thus no information about actual radiographic techniques is available. An alternative explanation is that the technologists were changing the density setting on the console, resulting in lower *S* values. We verified that the default density setting on the systems in question was zero.

Table 4 presents overall exposure indicator statistics for examinations performed at least 1,000 times throughout the data collection period. Several interesting trends were evident. First, it appears that the AEC systems on our cassette-based radiographic systems may be miscalibrated, resulting in overexposures. Views using manual exposure control exclusively, such as PORTABLE CHEST, ABDO MEN, LT DECUB, and ABDOMEN, RT DECUB, demonstrated mean and median *S* values close to the target of 200. However, views acquired predominantly under AEC, such as PELVIS, GENERAL, and FEMUR, PROXIMAL, demonstrated *S* values lower than the target of 200. Indeed, the mean *S* values for PORTABLE CHEST, ABDOMEN, LT DECUB, and ABDOMEN, RT DECUB were all significantly higher ($p<0.001$) than the mean *S* value for PELVIS, GENERAL. When stratified by clinical area, a surrogate for exposure control method, similar results were seen in the ABDOMEN, GENERAL data (Table 5). Three of the four main clinical areas depicted use AEC to acquire images, while the fourth area uses exclusively manual exposure control. All areas using AEC were characterized by mean *S* values that were significantly lower ($p<0.001$) than the area using manual exposure control. Thus, our radiographic equipment needs recalibration to make the AEC system more sensitive so that it will deliver less exposure. Also, while target *S* values of 200 were generally met, technologists consistently underexposed extremity examinations (TIB/FIB; FEMUR, DISTAL; HUMERUS; etc.), which have a target *S* value of 100. This can be attributed to several causes, including a lack of understanding of the difference in target *S* values for extremity ($S=100$) versus other ($S=200$) examinations, missing the extremity target because of consistent targeting of $S=200$ for bedside and other frequent examinations, or fear of exceeding the rejection criterion of $S=50$[1].

It is also interesting to note that the spread in *S* values, quantified by the coefficient of variation (COV), was generally less for images acquired using AEC compared to images acquired using manual exposure control (Tables 4 and 5). This is an expected result and is one of the distinct advantages of AEC over manual exposure control.

CONCLUSIONS

At first glance, it may seem that a reject analysis program is less useful for digital radiography, perhaps due to the stability of modern radiographic equipment and the absence of film processors. However, our data and that of others[8] demonstrate that a RAP is still necessary and useful in the era of digital imaging. It is vital, though, that the RAP be combined with an exposure analysis program, as digital radiography is not self-policing in terms of exposure as was screen–film radiography. When combined, the two programs are a powerful tool for quality assurance and staff education.

Using the methods and tools presented in this work, we were able to identify opportunities for both staff and student education. We also identi-

[1]The reason for this limit is the possibility of saturation/clipping in certain anatomical regions. In practice, we do not immediately reject every image with $S<50$; ideally, the images are evaluated for clipping or saturation prior to rejection. The choice of a lower limit for the *S* value involves consideration of the latitude (*L*) of the histogram of the values of interest (VOI). For example, if $L=2$ and $S=50$, an image pixel value of 511 would map to an exposure of 4 mR and the maximum VOI exposure would be 40 mR. However, certain details, such as the skin line, may be compromised with exposures beyond this point. If the latitude of the image is less, e.g., $L=1.5$ for an extremity image, larger overexposures can be tolerated without concern for clipping. If the latitude of the image is greater, e.g., $L=2.5$ for a chest image, clipping would be seen at lower exposure levels.

fied faults in our radiographic equipment, including miscalibrated AEC systems. An EAP is potentially useful for ongoing quality control of radiographic systems utilizing AEC. Finally, we have laid the framework for the automated collection, analysis, and presentation of data as part of both RAP and EAP.

We also propose that the results from our EAP demonstrate that frequent quality control testing, in particular exposure indicator calibration verification, may be warranted. Our results showed that *S* values and by extension patient exposures did not return to "baseline" levels for months after CR reader calibration. More frequent verification of the calibration would allow less time for the exposure indicator to deviate significantly from its calibrated value.

We are currently working to make our tool more useful by allowing supervisors to view the results of our statistical analyses in the HTTP interface and by automatically generating and distributing rejected image analysis and exposure analysis reports. In the future, we envision a server-based system that collects, analyzes, and archives RAP and EAP data from many different types of radiographic equipment and presents the results in a useful format. This type of system will be especially useful to participants in efforts such as the American College of Radiology's General Radiology Improvement Database,[27] which includes rejected images as one of its metrics. Such a system may also minimize scope creep, as the entire process would be automated and require minimal intervention from the informatics or medical physics departments. Rejected image analysis and exposure analysis reports could be automatically generated and delivered on a periodic basis, enabling radiology supervisors, department administrators, and medical physicists to perform their job duties more efficiently.

While we have presented many of the tools needed to accomplish this goal, it is still necessary for manufacturers to provide data in a common format that are accessible through hospital networks. One manufacturer has addressed this challenge with a digital dashboard for data collection and storage.[28] We have presented what we consider to be a minimal common dataset in this manuscript (Table 1), and we encourage manufacturers to provide at least these data in a widely usable, cross-platform format such as CSV. Finally, we encourage manufacturers to provide the means to access these data remotely to facilitate large-scale RAP and EAP at any institution that desires to set up such programs.

ACKNOWLEDGMENTS

The authors would like to thank Dawn Chalaire for her editorial assistance.

REFERENCES

1. United States Food and Drug Administration: Code of federal regulations, 21CFR900.12(e)(3)(ii), 2008
2. National Council on Radiation Protection and Measurements. Report 99. Quality assurance for diagnostic imaging. Bethesda: NCRP, 1988
3. American Association of Physicists in Medicine. Report 74. Quality control in diagnostic radiology. Madison: Medical Physics, 2002
4. American College of Radiology: ACR Technical Standard for Diagnostic Medical Physics Performance Monitoring of Radiographic and Fluoroscopic Equipment, Reston: ACR, 2006, pp. 1139–1142
5. Gray JE, Winkler NT, Stears J, Frank ED: Quality Control in Diagnostic Imaging, Gaithersburg: Aspen, 1983
6. Chu WK, Ferguson S, Wunder B, Smith R, Vanhoutte JJ: A two-year reject/retake profile analysis in pediatric radiology. Health Phys 42:53–59, 1982
7. GE Medical Systems: Revolution XQ/i digital radiographic imaging system. Pub. 98-5502:1–8, 1998
8. Honea R, Blado ME, Ma Y: Is reject analysis necessary after converting to computed radiography? J Digit Imaging 15 (Suppl 1):41–52, 2002
9. Nol J, Isouard G, Mirecki J: Digital repeat analysis; setup and operation. J Digit Imaging 19:159–166, 2006
10. Peer S, Peer R, Walcher M, Pohl M, Jaschke W: Comparative reject analysis in conventional film–screen and digital storage phosphor radiography. Eur Radiol, 9:1693–1696, 1999
11. Weatherburn GC, Bryan S, West M: A comparison of image reject rates when using film, hard copy computed radiography and soft copy images on picture archiving and communication systems (PACS) workstations. Br J Radiol 72:653–660, 1999
12. Prieto C, Vano E, Ten JI, et al: Image retake analysis in digital radiography using DICOM header information. J Digit Imaging 2008 doi:10.1007/s10278-008-9135-y
13. Foos DH, Sehnert WJ, Reiner B, et al: Digital radiography reject analysis: Data collection methodology, results, and recommendations from an in-depth investigation at two hospitals. J Digit Imaging 22:89–98, 2009
14. Polman R, Jones AK, Willis CE, Shepard SJ: Reject analysis tool. Proc SIIM 2008:38–40, 2008
15. Burkhart RL: Quality Assurance Programs for Diagnostic Radiology Facilities. In: U.S. Department of Health E, and Welfare ed: Washington, D.C.: Government Printing Office; 1980:21
16. Sagel SS, Jost RG, Glazer HS, et al: Digital mobile radiography. J Thorac Imag 5:36–48, 1990

17. Freedman M, Pe E, Mun SK: The potential for unnecessary patient exposure from the use of storage phosphor imaging systems. SPIE 1897:472–479, 1993

18. Gur D, Fuhman CR, Feist JH: Natural migration to a higher dose in CR imaging. Proceedings of the Eight European Congress of Radiology 154, 1993

19. Seibert JA, Shelton DK, Moore EH: Computed radiography X-ray exposure trends. Acad Radiol 3:313–318, 1996

20. Stewart BK, Kanal KM, Perdue JR, Mann FA: Computed radiography dose data mining and surveillance as an ongoing quality assurance improvement process. AJR 189:7–11, 2007

21. Practical Extraction and Report Language (Perl). www.perl.org. Accessed 22 June 2009.

22. Willis CE, Leckie RG, Carter JR, et al: Objective measures of quality assurance in a computed radiography-based radiology department. SPIE 2432:12, 1995

23. Crow EL, Shimizu K Eds. Lognormal Distributions: Theory and Applications, 1st ed. New York: CRC, 1988

24. Chauvenet WA: A Manual of Spherical and Practical Astronomy, 5th edition. Philadelphia: Lippincott, 1863

25. Carroll QB: Fuchs's Radiographic Exposure and Quality Control, 7th edition. Springfield: Thomas, 2003

26. Kuzmak PM, Dayhoff RE: Minimizing Digital Imaging and Communications in Medicine (DICOM) Modality Worklist patient/study selection errors. J Digit Imaging 14:153–157, 2001

27. American College of Radiology: General Radiology Improvement Database Metrics. https://nrdr.acr.org/portal/HELP/GRID/ACR_GRID_metrics.pdf. Accessed 5 February 2009

28. Minnigh TR, Gallet J: Maintaining quality control using a radiological digital X-ray dashboard. J Digit Imaging 22:84–88, 2009